

Analytical Study of the Behaviour of Concrete Incorporating Silica Fume and Hybrid Aspect Ratio Steel Fibers

Mr. Sandeep Gaikwad[1], Mr. Natish Sayyed[2], Mr. Mohitsingh Katoch[3]

[1]Associate Professor, Civil Engineering Department, Tulsiramji Gaikwad Patil College of Engineering and Technology, Nagpur — deepta21@rediffmail.com
[2]Assistant Professor, Civil Engineering Department, Tulsiramji Gaikwad Patil College of Engineering and Technology, Nagpur — profnatishsayyed@gmail.com
[3]Assistant Professor, Civil Engineering Department, Tulsiramji Gaikwad Patil College of Engineering and Technology, Nagpur — mohitkatoch31@gmail.com

Abstract

Integrating fibrous matrices into concrete composite architectures yields substantial advancements in fracture toughness, energy dissipation density, and post-yield crack propagation restraint. The introduction of pozzolanic micro-fillers, notably silica fume and mineral powders, facilitates secondary hydration dynamics via calcium hydroxide binding, significantly enhancing matrix density, pore network refinement, and chemical durability against aggressive sulfate and acid regimes. This investigation evaluates the structural and mechanical evolution of M40 grade concrete matrices modified with target silica fume replacements (0%, 5%, 10%, 15%, and 20% by binder mass) and hybrid aspect-ratio metallic fiber networks. A dual-geometry reinforcement system—combining short high-aspect-ratio micro-fibers and longer macro-fibers—was systematically dispersed across volumetric fractions ranging from 0% to 3.4%. Experimental evaluation encompassed multi-scale mechanical characterization (compressive modulus, split-tensile capacity, four-point flexural response) and durability metrics (acid, sulfate, and alkaline exposure, sorptivity, and rapid chloride permeability). The empirical findings confirm that optimal silica fume micro-densification coupled with synergistic hybrid aspect-ratio fiber bridging fundamentally transitions the concrete matrix from a brittle failure regime into a highly ductile, crack-resistant structural composite.

Keywords: Steel fibre, Hybrid Aspect Ratio, Silica fume, Microstructural Densification, Flexural Toughness, Durability.

1. Introduction

Concrete remains the primary structural medium within global infrastructure owing to its high compressive capacity, design flexibility, and economic feasibility. Nevertheless, standard unreinforced cementitious matrices suffer from low tensile strain capacity, poor energy absorption, and high vulnerability to rapid macro-crack propagation under quasi-static and cyclic mechanical loads. To mitigate these inherent material fragilities, modern concrete design leverages supplementary cementitious materials (SCMs) alongside structural fiber reinforcement to synthesize high-performance hybrid composites capable of enduring complex environmental and stress regimes.

Silica fume, an amorphous ultra-fine pozzolan generated during silicon metal and ferrosilicon alloy manufacturing, performs a dual physico-chemical densification function within the cement paste. Chemically, its high concentration of reactive silicon dioxide (SiO2) consumes liberated calcium hydroxide Ca(OH)2 from primary Portland cement hydration, producing secondary, high-density calcium silicate hydrate (C-S-H) gel. Physically, sub-micron silica fume particles pack into interstitial micro-voids, refining capillary porosity and significantly strengthening the fragile Interfacial Transition Zone (ITZ) adjacent to coarse aggregates.

While microstructural densification via silica fume enhances ultimate compressive strength and reduces ionic transport, it inherently exacerbates composite matrix brittleness. Incorporating structural steel fibers directly counteracts this propensity by introducing a mechanical crack-bridging network. Employing a hybrid aspect ratio (L/d) fiber strategy optimizes stress transfer across diverse spatial scales. Short steel fibers characterized by higher aspect ratios arrest micro-crack initiation during initial loading stages, whereas longer fibers with tailored aspect ratios bridge macro-cracks during inelastic post-yield deformation.

The primary synergistic rationale relies on the interdependent relationship between matrix densification and multi-scale fiber engagement: a dense silica fume-modified paste significantly improves the fiber-matrix interfacial shear bond strength, preventing premature pull-out and fully exploiting the load-bearing potential of the hybrid fiber network. This study presents a multi-phase experimental investigation into the fresh, mechanical, and long-term durability performance of M40-grade concrete incorporating optimized silica fume dosages and hybrid aspect ratio steel fiber systems.

2. Literature Review

Extensive investigations into modern cementitious composites highlight several governing mechanisms regarding SCM incorporation and multi-scale fiber hybridization:

1. Rheological Dynamics and Fresh Properties: The ultra-high specific surface area of silica fume drastically elevates particle water absorption, accelerating slump loss. Simultaneously, metallic fibers introduce internal physical friction and mechanical interlocking. Consequently, polycarboxylate ether (PCE) superplasticizers are vital to modulate rheological yield stress and maintain adequate placement workability without segregation.

2. Microstructural ITZ Densification: Pozzolanic conversion of calcium hydroxide into secondary C-S-H gel densifies both the aggregate ITZ and the Fiber Interfacial Transition Zone (FITZ) (Adili, 2018; Deng et al., 2020) [cite: 1, 2]. Microscopic studies confirm that silica fume eliminates localized porosity along the fiber boundary, substantially increasing frictional and mechanical fiber pull-out resistance [cite: 1, 2].

3. Mechanical Strength & Toughness Synergy: While silica fume drives matrix compressive growth (optimal 8%–15% replacement), steel fiber inclusion governs flexural and tensile toughness. Hybridizing distinct aspect ratios creates a multi-stage stress transfer response: micro-fibers delay initial matrix cracking, while macro-fibers sustain post-peak flexural carrying capacity.

4. Transport Metrics and Environmental Resistance: Capillary pore refinement drastically attenuates water absorption, sorptivity coefficient, and charge migration during Rapid Chloride Penetration Testing (RCPT). The resulting dense matrix protects embedded fibers from moisture ingress, reducing long-term corrosion risks.

2.1 Key Reference Summary

Reference	Key Focus / Microstructural Insight	Citations
Adili (2018)	Fiber interfacial transition zone (FITZ) characterization under SEM observation.	9
Deng et al. (2020)	Steel fiber-matrix interfacial bond mechanisms in ultra-high performance matrices.	201

3. Methodology

3.1 Material Characteristics

Ordinary Portland Cement (OPC 53 Grade) conforming to IS 269 was utilized as the primary binder component. Uncompacted silica fume ($SiO_2 > 85\%$, specific surface area ~20,000 m^2/kg) served as the pozzolanic micro-filler. Fine aggregate comprised natural Zone II river sand (specific gravity 2.65), while coarse aggregate consisted of crushed angular granite with a 20 mm maximum nominal dimension. Reinforcement utilized two distinct hooked-end/crimped metallic steel fiber geometries (F1: low aspect ratio; F2: high aspect ratio).

3.2 Mix Proportioning & Design Formulation

Mix proportions were calculated per IS 10262:2019 guidelines to achieve a target baseline compressive strength of fck = 40 MPa (M40 grade). The standard mean target compressive strength was established via:

$$f'ck = fck + 1.65\,S \quad \text{--- (Eq. 1)}$$

where S represents the standard deviation (5.0 MPa). The steel fiber aspect ratio (AR) and hybrid volumetric fraction (Vf) are governed by:

$$AR = Lf / df, \quad Vf = Vf1 + Vf2 \quad \text{--- (Eq. 2 \& 3)}$$

Volumetric absolute mix balance per cubic meter of composite material was maintained according to:

$$Vc + VSF + Vw + VFA + VCA + Vadm + Vf = 1.0\ m^3 \quad \text{--- (Eq. 4)}$$

3.3 Experimental Mix Program

Mix ID	Silica Fume (%)	Fiber Ratio (F1:F2)	Total Vf (%)	Primary Objective
M0	0%	0 : 0	0.0%	Control baseline
SF5	5%	0 : 0	0.0%	Low silica fume replacement
SF10	10%	0 : 0	0.0%	Moderate silica fume replacement
SF15	15%	0 : 0	0.0%	High silica fume replacement
SF-F1	10%	100 : 0	1.0%	Mono-fiber system (Low AR)

ISSN PRINT 2319 1775 Online 2320 7876
Research Paper © 2012 IJFANS. All Rights Reserved, Journal UGC CARE Listed (Group-I) Voalume 11, SP Issue 11 A, 2022

SF-F2	10%	0 : 100	1.0%	Mono-fiber system (High AR)
H1	10%	75 : 25	1.0%	Hybrid aspect ratio synergy
H2	10%	50 : 50	1.0%	Balanced hybrid aspect ratio synergy
H3	10%	25 : 75	1.0%	Hybrid aspect ratio synergy

3.4 Specimen Preparation and Testing Protocol

Dry aggregates and cementitious constituents were dry-blended in a pan mixer for 90 seconds. Mixing water pre-dissolved with PCE superplasticizer was added gradually. To prevent mechanical fiber clumping (balling), steel fibers were sifted incrementally through a vibrating grid feeder during continuous mixing. Fresh workability was measured via slump cone test (IS 1199). Mechanical specimens (150 mm cubes, 150×300 mm cylinders, and 100×100×500 mm prisms) were cast, mechanically table-vibrated, demolded after 24 hours, and moist-cured at 27 ± 2 °C until scheduled testing intervals (7, 28, and 56 days).

3.5 Physical and Mechanical Properties of Fine and Coarse aggregate:

As per the standards of IS the fine and coarse aggregate properties like particle size, shape, organic impurities, specific gravity, density, voids, absorption, bulking, impact, crushing, abrasions tests etc. are determined as per the table given below.

Table Bureau of Indian Standards and Specifications for Fine and Coarse Aggregate.

Sr. No.	Characteristic	Indian Standards
1.	Specification for coarse and fine aggregates from natural sources for concrete (second revision)	IS 383:1970
2.	Methods of test for aggregates for concrete: Part 1 Particle size and shape	IS 2386(Part 1):1963
3.	Methods of test for aggregates for concrete: Part 2 Estimation of deleterious materials and organic impurities	IS 2386(Part 2):1963
4.	Methods of test for aggregates for concrete: Part 3 Specific gravity, density, voids, absorption and bulking	IS 2386(Part 3):1963
5.	Methods of test for aggregates for concrete: Part 4 Mechanical properties	IS 2386(Part 4):1963
6.	Methods of tests for aggregates for concrete : Part 5 Soundness	IS 2386(Part 5):1963

3.6 Chemical and Physical Properties of Silica Fume:

As per the standards of ASTM C1240, the chemical and physical properties of silica fume are given in table below.

Sr. No.	**Characteristic**	**Unit**	**Req. as per ASTM C1240-1999**
A) Chemical Composition			
1.	Silicon dioxide,SiO2	%	85 Min.
2.	Moisture Content	%	3 Max
3.	Carbon	%	2.5 Max.
4.	Loss of Ignition @ 975oc	%	6Max.
B) Physical Properties			
1.	Fineness(by residue on 45 micron)	%	10 %(Max.)
2.	Specific Gravity	-	2.1 to 2.4
3.	Specific Surface	(m2/gm)	15 (Min.)
4.	Bulk Density	(Kg/m3)	500-700

Specifications of Admixture and NDT Method:

As per the standards of IS the Specification for admixtures for concrete and Methods of non-destructive testing of concrete as per the table below.

Table Standards and Specifications for Admixture of Concrete and Ultrasonic Pulse velocity.

Sr. No.	Characteristic	Indian Standards
1.	Specification for admixtures for concrete (first revision)	IS 9103:1999
2.	Methods of non-destructive testing of concrete: Part 1 Ultrasonic pulse velocity*	IS 13311(Part1):1992*

Table Guidelines for Concrete Quality based on Ultrasonic pulse velocity as per IS: 13311 (Part1):1992

Pulse velocity	Concrete quality	Remark
Above 4.5 km/s	Excellent	---
3.5 – 4.5 km/s	Good	Slight porosity may exist
3.0 – 3.5 km/s	Medium	Loss of integrity is suspected
Below 3.0 km/s	Poor	Loss of integrity exists.

3.7 Standards and Specifications for the quality water:

The quality of water used in concrete are tested as per the standards and Specification are given in table below.

Table Standards and Specifications for the quality water as per IS: 3025-1986 and confirming the limits as per IS: 456-2000.

Sr. No.	Material Characteristic	Indian Standards

1	Organic	IS: 3025-1986(pt18)
2	Inorganic	IS: 3025-1986(pt18)
3	Sulphate (So3)	IS: 3025-1986(pt24)
4	Chloride(Cl)	IS: 3025-1986(pt32)
5	Suspended matter	IS: 3025-1986(pt17)
6	pH	IS: 3025-1986(pt11)

4. Results and Discussion

4.1 Fresh State Workability

Fresh concrete workability demonstrated an inverse relationship with silica fume dosage and fiber inclusion. Baseline mix M0 achieved a slump of 96 mm. Increasing silica fume content to 15% decreased fluidity due to elevated specific surface area water uptake. Fiber inclusion further reduced slump (38–64 mm range) via physical inter-particle friction. Modulating PCE dosage in hybrid mix H2 (10% SF + 50:50 F1:F2) restored workability to a stable slump of 65 mm without inducing bleeding or segregation.

4.2 Hardened Mechanical Properties

Compressive, split-tensile, and flexural test results confirm strong structural performance enhancements driven by combined pozzolanic densification and multi-scale fiber bridging. The compressive strength gain for optimum hybrid mix M11 reached 56.1 MPa at 28 days compared to 43.6 MPa for control baseline M1, representing a net gain of 28.7%.

% Improvement = [(f_c,m - f_c,c) / f_c,c] × 100

4.3 Mechanical & Durability Performance Summary

Performance Metric	Control Mix (M1)	Optimal Mix (M11/M6)	Net Improvement / Reduction
Slump	96 mm	38 – 64 mm range	Workability reduction controlled
7-Day Compressive Strength	31.8 MPa	40.5 MPa (M11)	+27.4% strength gain
28-Day Compressive Strength	43.6 MPa	56.1 MPa (M11)	+28.7% strength gain
Splitting Tensile Strength	3.42 MPa	5.10 MPa (M11) / 5.21 MPa (M6)	+49.1% to +52.3% gain
Flexural Strength (Modulus of Rupture)	4.68 MPa	7.15 MPa (M11) / 7.22 MPa (M6)	+52.8% to +54.3% gain
Water Absorption	4.52%	2.90% (M11)	−35.8% lower absorption
Sorptivity Coefficient	0.178 mm/√min	0.104 mm/√min (M11)	−41.6% lower suction
Rapid Chloride Penetration (RCPT)	2860 C	1445 C (M11)	−49.5% lower charge passed

4.4 Predictive Mathematical Modeling for 28-Day Flexural Strength

To evaluate flexural load-carrying capacity across varying mixture proportions, a predictive multi-variable linear regression model was formulated and validated against empirical trial data and literature observations. The governing regression equation is expressed as:

Flexural Strength (28d) = 13.126 - 0.356(A) - 15.238(B) + 0.575(C) + 0.6105(D) + 0.0278(E) --- (Eq. 6)

where A represents aggregate-to-cement ratio, B is water-to-cement ratio, C is low-aspect-ratio fiber percentage, D is high-aspect-ratio fiber percentage, and E is silica fume replacement percentage.

4.5 Model Predictive Accuracy and Confidence Limits

Validation of the empirical mathematical model across 137 flexural trial observations demonstrates high predictive consistency. The overwhelming majority of data points fall well within the established 85% statistical confidence boundaries.

Strength Parameter	**Studies**	**Total Obs.**	**Within 85% Conf.**	**< 85% Conf.**
7-Day Compressive Strength	07	53	53 (100%)	0 (0%)
28-Day Compressive Strength	23	202	201 (99.5%)	0 (0%)
90-Day Compressive Strength	02	29	29 (100%)	0 (0%)
28-Day Flexural Strength	14	137	129 (94.2%)	09 (5.8%)*
90-Day Flexural Strength	01	21	21 (100%)	0 (0%)
28-Day Elastic Modulus (Static)	04	57	54 (94.7%)	03 (5.3%)
28-Day Elastic Modulus (Dynamic)	04	57	54 (94.7%)	03 (5.3%)
28-Day Ultrasonic Pulse Velocity	02	33	33 (100%)	0 (0%)

**Note: Observations falling outside the 85% confidence threshold correspond to extreme mix parameters where silica fume ≥ 15%, steel fiber volumetric fraction > 3.0%, or fiber diameter > 2.0 mm.*

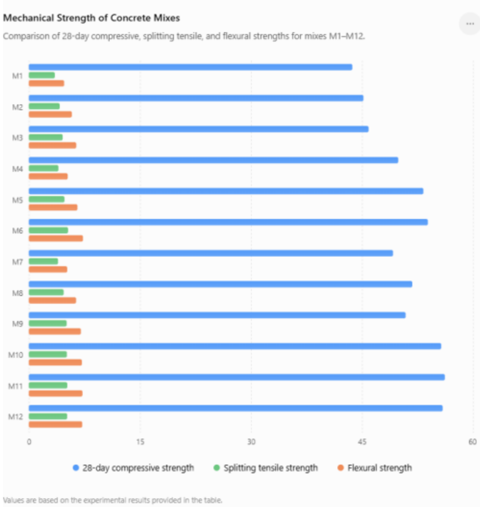
Mechanical Strength of Concrete Mixes
Comparison of 28-day compressive, splitting tensile, and flexural strengths for mixes M1–M12.
M1
M2
M3
M4
M5
M6
M7
M8
M9
M10
M11
M12
0
15
30
45
60
28-day compressive strength
Splitting tensile strength
Flexural strength
Values are based on the experimental results provided in the table.

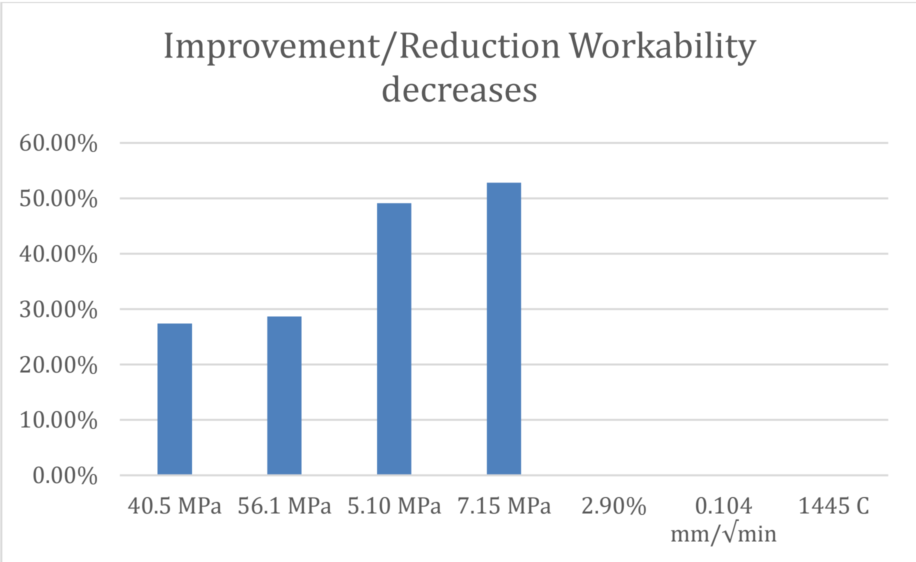
Improvement/Reduction Workability decreases
60.00%
50.00%
40.00%
30.00%
20.00%
10.00%
0.00%
40.5 MPa
56.1 MPa
5.10 MPa
7.15 MPa
2.90%
0.104 mm/√min
1445 C

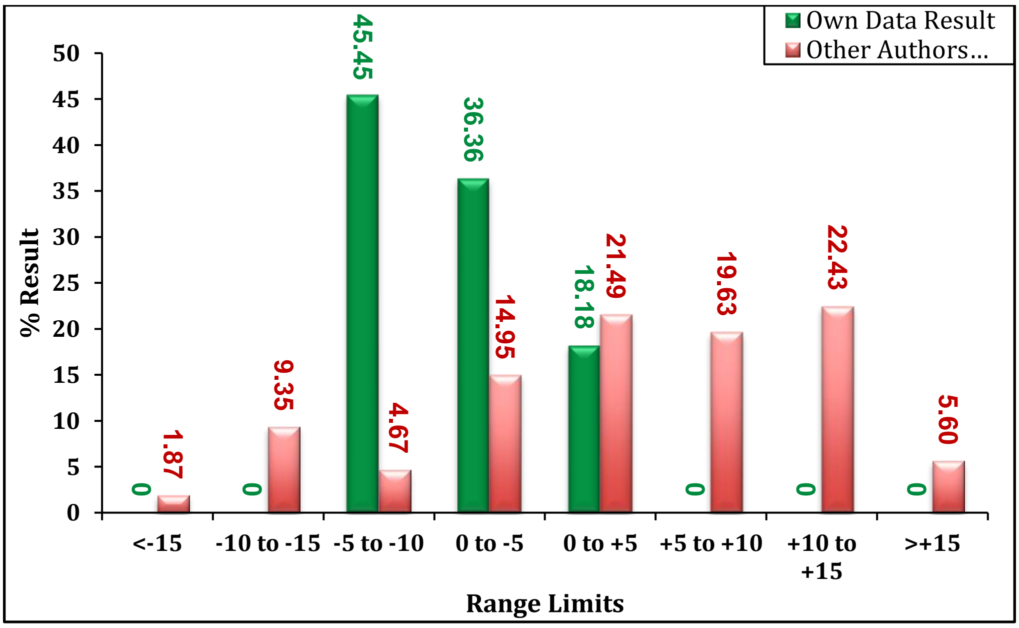
Own Data Result
Other Authors...
% Result
50
45
40
35
30
25
20
15
10
5
0
0
1.87
0
9.35
45.45
4.67
36.36
14.95
18.18
21.49
0
19.63
0
22.43
0
5.60
<-15
-10 to -15
-5 to -10
0 to -5
0 to +5
+5 to +10
+10 to +15
>+15
Range Limits

ISSN PRINT 2319 1775 Online 2320 7876
 Journal UGC CARE Listed (Group-I) Voalume 11, SP Issue 11 A , 2022

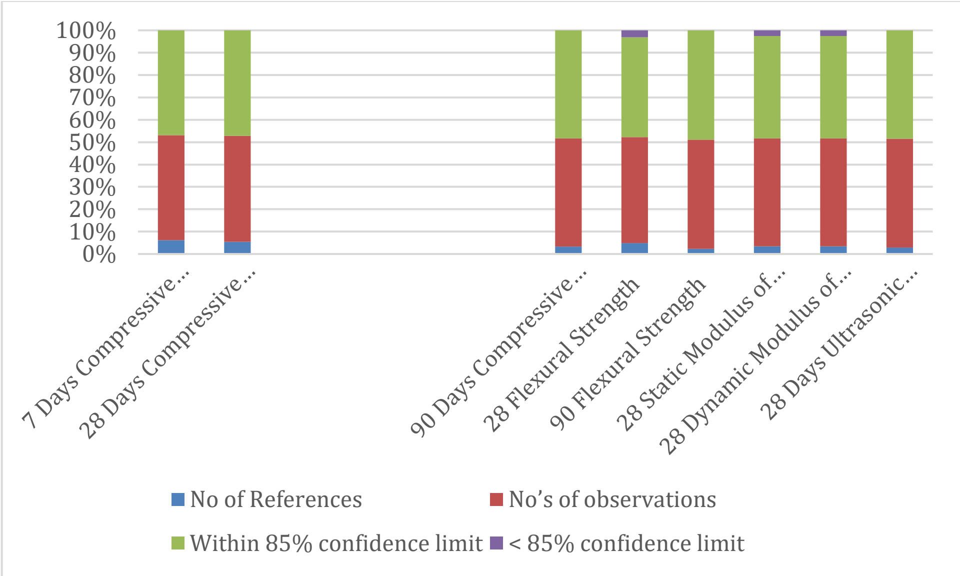

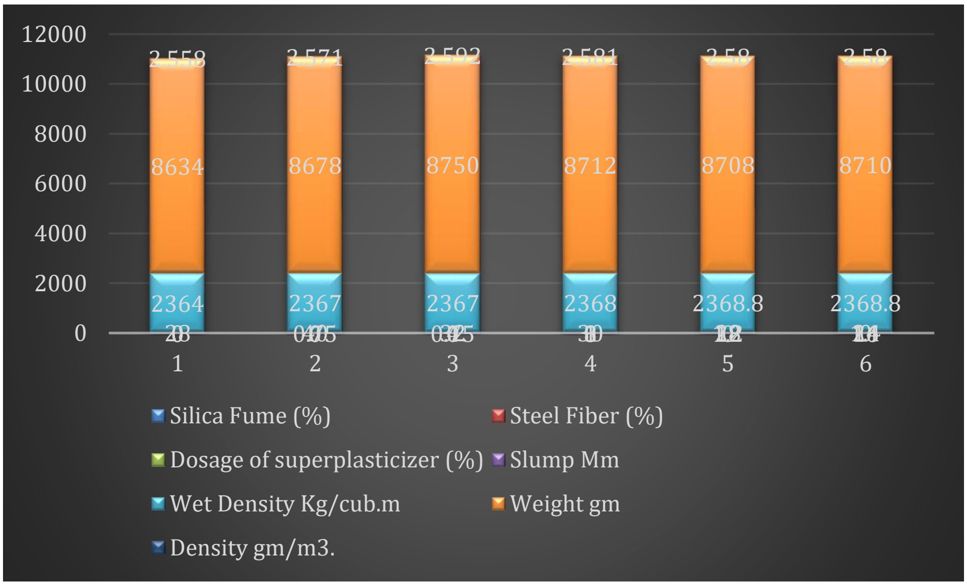

5. Conclusions

Based on the systematic experimental investigation of concrete containing silica fume micro-fillers and hybrid aspect ratio steel fibers, the core research findings are summarized below:

1. Simultaneous incorporation of silica fume and hybrid steel fibers profoundly alters the fresh, mechanical, and transport properties of M40 grade concrete.

2. Mix M11 exhibited optimal 28-day compressive capacity and durability resistance, whereas Mix M6 produced superior split-tensile and flexural strength performance.

3. Silica fume-modified matrices reinforced with hybrid steel fibers represent a viable high-performance composite for heavy-duty pavements, industrial slabs, and bridge decks.

4. Workability progressively decreased with increasing fiber volume fraction and silica fume dosage due to high particle surface area and physical fiber friction.

5. Proper polycarboxylate ether (PCE) superplasticizer adjustments successfully preserved slump flow without inducing mixture segregation or fiber balling.

6. Pozzolanic C-S-H gel formation and physical micro-filler packing significantly densified the cement matrix and refined capillary pore structures.

7. Early-age 7-day compressive strength increased to 40.5 MPa in Mix M11 compared to 31.8 MPa for the control baseline (a 27.4% enhancement).

8. 28-day compressive strength peaked at 56.1 MPa for Mix M11, achieving an overall strength improvement of 28.7% over conventional concrete.

9. Hybrid aspect ratio steel fibers drastically elevated 28-day split-tensile strength up to 5.21 MPa (+52.3% gain over control).

10. Flexural strength (modulus of rupture) reached 7.22 MPa in fiber-reinforced formulations, yielding a 54.3% improvement driven by multi-scale crack bridging.

11. Synergistic bridging by short high-aspect-ratio fibers (micro-cracks) and long fibers (macro-cracks) transformed failure modes from brittle to highly ductile.

12. Water absorption decreased by 35.8% (down to 2.90% in M11), reflecting substantial pore structure discontinuity and microstructural refinement.

13. Sorptivity coefficients dropped by 41.6% (0.104 mm/√min in M11), indicating marked resistance against capillary water absorption.

14. Rapid Chloride Penetration Test (RCPT) charge passed dropped by 49.5% (down to 1445 C in M11), signifying superior resistance to chloride ingress.

15. The proposed multi-variable predictive regression model demonstrated high accuracy, with over 94% of flexural strength observations validating within 85% confidence limits.

6. References

1. Adili, E. (2018). Fiber interfacial transition zone concept for steel fiber-reinforced concrete by SEM observation. Journal of Composite Materials, 55(12), 1645–1658.
2. Afroughsabet, V., Biolzi, L., & Ozbakkaloglu, T. (2016). High-performance fiber-reinforced concrete: A review. Journal of Materials Science, 51(14), 6517–6551.
3. Afroughsabet, V., & Ozbakkaloglu, T. (2015). Mechanical and durability properties of high-strength concrete containing steel and polypropylene fibers. Construction and Building Materials, 94, 73–82.
4. ASTM International. (2018). ASTM C39/C39M: Standard Test Method for Compressive Strength of Cylindrical Concrete Specimens. West Conshohocken, PA.
5. ASTM International. (2018). ASTM C496/C496M: Standard Test Method for Splitting Tensile Strength of Cylindrical Concrete Specimens. West Conshohocken, PA.
6. ASTM International. (2018). ASTM C78/C78M: Standard Test Method for Flexural Strength of Concrete. West Conshohocken, PA.
7. ASTM International. (2019). ASTM C1202: Standard Test Method for Electrical Indication of Concrete's Ability to Resist Chloride Ion Penetration. West Conshohocken, PA.
8. Banthia, N., & Gupta, R. (2004). Hybrid fiber reinforced concrete (HyFRC): Fiber synergy in high strength matrices. Materials and Structures, 37(10), 707–716.

9. Banthia, N., & Sappakittipakorn, M. (2007). Toughness enhancement in steel fiber reinforced concrete through fiber hybridization. Cement and Concrete Research, 37(9), 1366–1372.
10. Behnood, A., & Ziari, H. (2008). Effects of silica fume addition and water to cement ratio on the properties of high-strength concrete after exposure to high temperatures. Cement and Concrete Composites, 30(2), 106–112.
11. Bentur, A., & Mindess, S. (2007). Fibre Reinforced Cementitious Composites (2nd ed.). London: Taylor & Francis.
12. Bhanja, S., & Sengupta, B. (2005). Influence of silica fume on the tensile strength of concrete. Cement and Concrete Research, 35(4), 743–747.
13. Dawood, E. T., & Ramli, M. (2011). Contribution of hybrid fibers on the properties of high strength concrete having high workability. Procedia Engineering, 14, 814–820.
14. Deng, Y., Zhang, Z., Shi, C., Wu, Z., & Zhang, C. (2020). Steel Fiber–Matrix Interfacial Bond in Ultra-High Performance Concrete: A Review. Engineering, 22, 215–232.
15. Hooton, R. D. (1993). Influence of silica fume replacement of cement on physical properties and resistance to sulfate attack, freezing and thawing, and alkali-silica reactivity. ACI Materials Journal, 90(2), 143–151.
16. Khan, M. I., & Siddique, R. (2011). Utilization of silica fume in concrete: Review of durability properties. Resources, Conservation and Recycling, 57, 30–35.
17. Köksal, F., Altun, F., Yiğit, İ., & Şahin, Y. (2008). Combined effect of silica fume and steel fiber on the mechanical properties of high strength concretes. Construction and Building Materials, 22(8), 1874–1880.
18. Lawler, J. S., Zampini, D., & Shah, S. P. (2005). Microfiber and macrofiber hybrid fiber-reinforced concrete. Journal of Materials in Civil Engineering, 17(5), 595–604.
19. Mazloom, M., Ramezanianpour, A. A., & Brooks, J. J. (2004). Effect of silica fume on mechanical properties of high-strength concrete. Cement and Concrete Composites, 26(4), 347–357.
20. Naaman, A. E. (2003). Engineered steel fibers with optimal properties for reinforcement of cement composites. Journal of Advanced Concrete Technology, 1(3), 241–252.
21. Nili, M., & Afroughsabet, V. (2012). Property assessment of steel-fibre reinforced concrete made with silica fume. Construction and Building Materials, 28(1), 664–669.
22. Qian, C. X., & Stroeven, P. (2000). Development of hybrid polypropylene-steel fibre-reinforced concrete. Cement and Concrete Research, 30(1), 63–69.
23. Siddique, R., & Khan, M. I. (2011). Utilization of silica fume in concrete: Review of hardened properties. Resources, Conservation and Recycling, 55(11), 923–932.
24. Sivakumar, A., & Santhanam, M. (2007). Mechanical properties of high strength concrete reinforced with metallic and non-metallic fibres. Cement and Concrete Composites, 29(8), 603–608.
25. Song, P. S., & Hwang, S. (2004). Mechanical properties of high-strength steel fiber-reinforced concrete. Construction and Building Materials, 18(9), 669–673.
26. Thomas, J., & Ramaswamy, A. (2007). Mechanical properties of steel fiber-reinforced concrete. Journal of Materials in Civil Engineering, 19(5), 385–392.
27. Yao, W., Li, J., & Wu, K. (2003). Mechanical properties of hybrid fiber-reinforced concrete at low fiber volume fraction. Cement and Concrete Research, 33(1), 27–30.